circRNA-0002109 promotes glioma malignant progression via modulating the miR-129-5P/EMP2 axis

Haibin Xia,[1,4,5] Boyang Liu,[2,5] Nanxiang Shen,[1] Jinhua Xue,[3] Siyu Chen,[1] Hongbo Guo,[2] and Xiaozhong Zhou[4]

[1]Institute of Neuroscience and the Second Affiliated Hospital of Guangzhou Medical University, 250 Chang-gang East Road, Guangzhou 510260, China; [2]Neurosurgery Center, The National Key Clinical Specialty, The Engineering Technology Research Center of Education Ministry of China on Diagnosis and Treatment of Cerebrovascular Disease, Guangdong Provincial Key Laboratory on Brain Function Repair and Regeneration, The Neurosurgery Institute of Guangdong Province, Zhujiang Hospital, Southern Medical University, Guangzhou 510282, China; [3]Department of Physiology, School of Basic Medical Sciences, Gannan Medical University, Ganzhou 341000, China; [4]Trauma Center, First Affiliated Hospital of Gannan Medical University, Ganzhou 341000, China

Glioma is a common intracranial malignant tumor with high mortality and high recurrence rate. In recent years, increasing evidence has demonstrated that circular RNAs (circRNAs) are potential biomarkers and therapeutic targets for many tumors. However, the role of circRNAs in glioma remains unclear. In this study, we found that circRNA-0002109 was highly expressed in glioma tissues and cell lines. Downregulation of circRNA-0002109 expression inhibited the proliferation, migration, and invasion of glioma cells and inhibited the malignant progression of tumors in vivo. Investigations into the relevant mechanisms showed that circRNA-0002109 upregulated the expression of EMP2 through endogenous competitive binding of microRNA-129-5P (miR-129-5P), which partially alleviated the inhibitory effect of miR-129-5P on epithelial membrane protein-2 (EMP2) and ultimately promoted the malignant development of glioma. Our results indicate that circRNA-0002109 plays an important role in the proliferation, invasion, and migration of glioma cells by regulating the miR-129-5P/EMP2 axis, which provides a new potential therapeutic target for glioma.

INTRODUCTION

Glioma is the most common primary intracranial malignant tumor,[1] with a high recurrence rate even after surgery, radiotherapy, chemotherapy, and other comprehensive treatments.[2,3] According to the 2007 World Health Organization (WHO) criteria, glioblastoma multiforme (GBM) is a grade IV tumor and is the most malignant type of glioma.[4] However, even after current advanced treatment, patients diagnosed with GBM have a median survival of less than 16 months.[5,6] Therefore, we urgently need to explore the potential molecular mechanisms of glioma development, especially GBM, and to develop more effective treatment measures.

In recent years, circular RNAs (circRNAs) have attracted much attention and become a research hotspot in various disease fields, especially in cancer research.[7–9] circRNAs are closed-loop structures generated by reverse splicing of precursor mRNAs, resulting in the lack of a 5′-end cap or a 3′-terminal poly(A) tail; this decreases the degradation rate of circRNAs.[10,11] Therefore, circRNAs have a unique advantage as a disease diagnostic marker and treatment target.[12] Recently, studies have shown that circRNAs can inhibit the activity of specific downstream microRNAs (miRNAs) and consequently indirectly regulate the expression of miRNA target genes, thus functioning as competing endogenous RNAs (ceRNAs).[13,14] In addition, circRNAs can act as RNA-binding protein sponges and have the ability to encode proteins.[15–17] Existing evidence has also shown that the imbalanced expression of circRNAs can greatly affect the occurrence and development of tumors by regulating biological processes, including the proliferation, migration, metastasis, and invasion of tumor cells. For example, circBFAR promotes the progression of pancreatic ductal carcinoma by regulating the microRNA-34b-5P (miR-34b-5P)/Met/AKT axis.[18] circFNDC3B encodes a newly identified protein, circfNDC3B-218AA, which inhibits the proliferation and metastasis of colon cancer.[19] However, little is known about the regulatory mechanisms of circRNAs in glioma.

As a cell surface protein, epithelial membrane protein-2 (EMP2) is one of the growth arrest-specific gene 3/peripheral myelin protein 22 (GAS3/PMP22) tetraspan proteins, and it is closely involved in cell proliferation, migration, and adhesion.[20] Studies have shown that EMP2 expression is upregulated in various tumors and associated with poor prognosis.[21,22] In recent years, EMP2 has become a
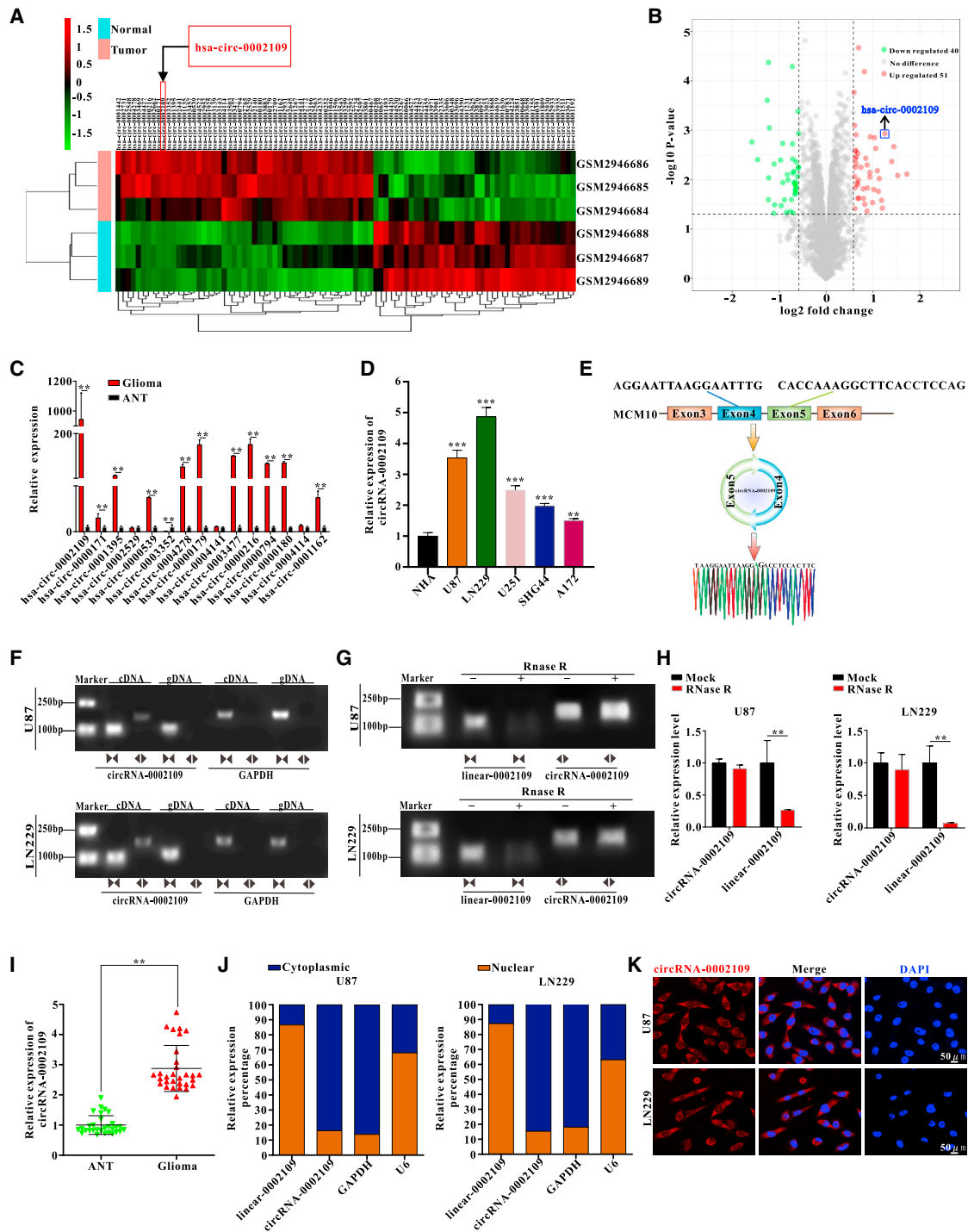
Figure 1. circRNA-0002109 is upregulated in glioma tissues and cell lines

(A) Heatmap and (B) volcano map of differentially expressed circRNAs between glioma tissues and paired adjacent normal tissues (ANTs) in GSE109569 microarray. (C) The expression levels of 15 circRNAs were determined by RT-qPCR in ANT and glioma tissues. (D) The circRNA-0002109 expression level in NHA cell lines and human glioma cell lines (U87, LN229, U251, SHG44, A172). (E) The circRNA-0002109 was back-spliced by exon 4 and exon 5 of MCM10 and verified by Sanger sequencing. (F) Agarose gel electrophoresis showed that only divergent primers amplified circRNA-0002109 in cDNA. GAPDH served as a negative control. (G and H) Validation of circRNA-0002109

(legend continued on next page)

hotspot in cancer research, especially in glioma research because of its potential as a biomarker.[23,24] However, little is known about the regulatory mechanisms of EMP2 in gliomas.

In this study, we selected circRNA-0002109 by bioinformatic analysis and identified that circRNA-0002109 acts as a sponge for miR-129-5P to indirectly regulate the expression of EMP2 in gliomas. Then, through *in vitro* and *in vivo* experiments, we demonstrated that circRNA-0002109 played a role in the malignant progression of glioma by regulating the miR-129-5P/EMP2 axis. Our study provides evidence for a new and promising target for the treatment of glioma.

RESULTS

circRNA-0002109 is upregulated in glioma tissues and cell lines

Upon analyzing the circRNA microarray in GEO datasets (GEO: GSE109569),[25] we identified 4,423 circRNAs in three pairs of glioma specimens (three glioma tissues and three matching tumor-adjacent tissues). With a p value less than 0.05 and |log2fold-change| greater than 0.58 as the threshold, 91 differentially expressed circRNAs, including 51 upregulated and 40 downregulated circRNAs, were identified (Table S1). We constructed a heatmap and volcano map to show the differentially expressed circRNAs (Figures 1A and 1B). Among the 51 upregulated circRNAs, 15 circRNAs had a p value less than 0.01 and |log2fold-change| greater than 1.0 (Table S2). The expression levels of these 15 circRNAs in glioma tissues were further verified by RT-qPCR analysis. Compared with that in the corresponding tumor-adjacent normal tissues (N = 3), the expression level of hsa-circ-0002109 in glioma tissues was the most abundant (Figure 1C). Therefore, we focused on hsa-circ-0002109, and we renamed it circRNA-0002109 in this study. RT-qPCR analysis further showed that the expression level of circRNA-0002109 in glioma cell lines was higher than that in normal cell lines. Moreover, circRNA-0002109 expression levels in U87 and LN229 cell lines were higher than those in other glioma cell lines, so we selected U87 and LN229 cell lines for subsequent experiments (Figure 1D). Analysis of the circBase database (http://www.circbase.org/) revealed that circRNA-0002109 was formed by head-to-tail splicing of exons 4 and 5 of Minichromosome Maintenance 10 Replication Initiation Factor (MCM10), and its length was 246 nt. The head-to-tail splicing of circRNA-0002109 was further verified by Sanger sequencing (Figure 1E). All the results indicate that circRNA-0002109 expression is upregulated in glioma tissues and cells.

Next, we designed a convergent primer for linear-0002109 and a divergent primer for circRNA-0002109 and performed electrophoresis with cDNA and genomic DNA (gDNA) as the PCR templates. The results showed that the divergent primers only amplified circRNA-0002109 from cDNA, and no amplified products were found in samples containing gDNA (Figure 1F). Glioma cells were pretreated with RNase R to detect the stability of circRNA-0002109.

Electrophoresis results showed that circRNA-0002109 was resistant to RNase R digestion, while the expression level of linear-0002109 decreased (Figures 1G and 1H). We then detected the expression level of circRNA-0002109 in glioma tissues and matched tumor-adjacent normal tissues (N = 30) and found that the abundance of circRNA-0002109 in glioma tissues was significantly higher than that in tumor-adjacent normal tissues (Figure 1I), indicating that the expression of circRNA-0002109 is correlated with glioma. Finally, we detected the subcellular localization of circRNA-0002109 and conducted RT-qPCR analysis on the nuclear and cytoplasmic fractions of glioma cells, which showed that circRNA-0002109 was mainly localized to the cytoplasm (Figure 1J). Fluorescence in situ hybridization (FISH) experiments further confirmed this conclusion (Figure 1K). These data illustrated that circRNA-0002109 upregulation is common in glioma and may have a vital role in the progression of glioma.

High expression of circRNA-0002109 promotes the proliferation, migration, and invasion of glioma cells

To evaluate the role of circRNA-0002109 in glioma, lentiviral vectors were constructed to knock down or overexpress circRNA-0002109 and were transduced into U87 and LN229 cells. Then, the transduction efficiency was verified by RT-qPCR analysis, which showed that sh-circRNA-0002109 #1 had the strongest knockdown efficiency, while the level of linear-0002109 was not significantly changed. Thus, in subsequent studies, we performed knockdown experiments using sh-circRNA-0002109 #1 (Figures 2A and S1A). Next, we evaluated the effect of circRNA-0002109 on cell proliferation with the CCK-8 and 5-ethynyl-2′-deoxyuridine (EdU) staining assays, which revealed that downregulation of circRNA-0002109 could impair the proliferation ability, while overexpression of circRNA-0002109 could accelerate proliferation (Figures 2B–2D). The transwell assay results showed that circRNA-0002109 knockdown significantly inhibited the migration and invasion of U87 and LN229 cells, while overexpression of circRNA-0002109 promoted their migration and invasion (Figures 2E and 2F). Finally, we detected the effect of circRNA-0002109 on the changes in the protein expression of epithelial-mesenchymal transition (EMT) marker genes by western blotting. The results showed that knockdown of circRNA-0002109 decreased the protein levels of N-cadherin, Snail, Slug, and Vimentin, and increased E-cadherin protein levels, while overexpression of circRNA-0002109 had the opposite results (Figure 2G). Taken together, these data indicate that circRNA-0002109 has a carcinogenic effect in glioma cells, and high levels of circRNA-0002109 expression can enhance the proliferation, migration, and invasion of glioma cells.

CircRNA-0002109 functions as a sponge for miR-129-5P in glioma cells

Studies have shown that circRNAs mainly function as a sponge in the cytoplasm to regulate their downstream miRNAs. To further explore such downstream miRNAs of circRNA-0002109, we

stability by RNase R treatment and RT-qPCR analysis. (I) Relative circRNA-0002109 expression levels in paired ANTs (n = 30) and glioma tissues (n = 30). (J and K) Nuclear-cytoplasmic separation and FISH shown subcellular localization of circRNA-0002109. Scale bars, 50 μm. Data are presented as mean ± SD of three independent experiments. **p < 0.01; ***p < 0.001.
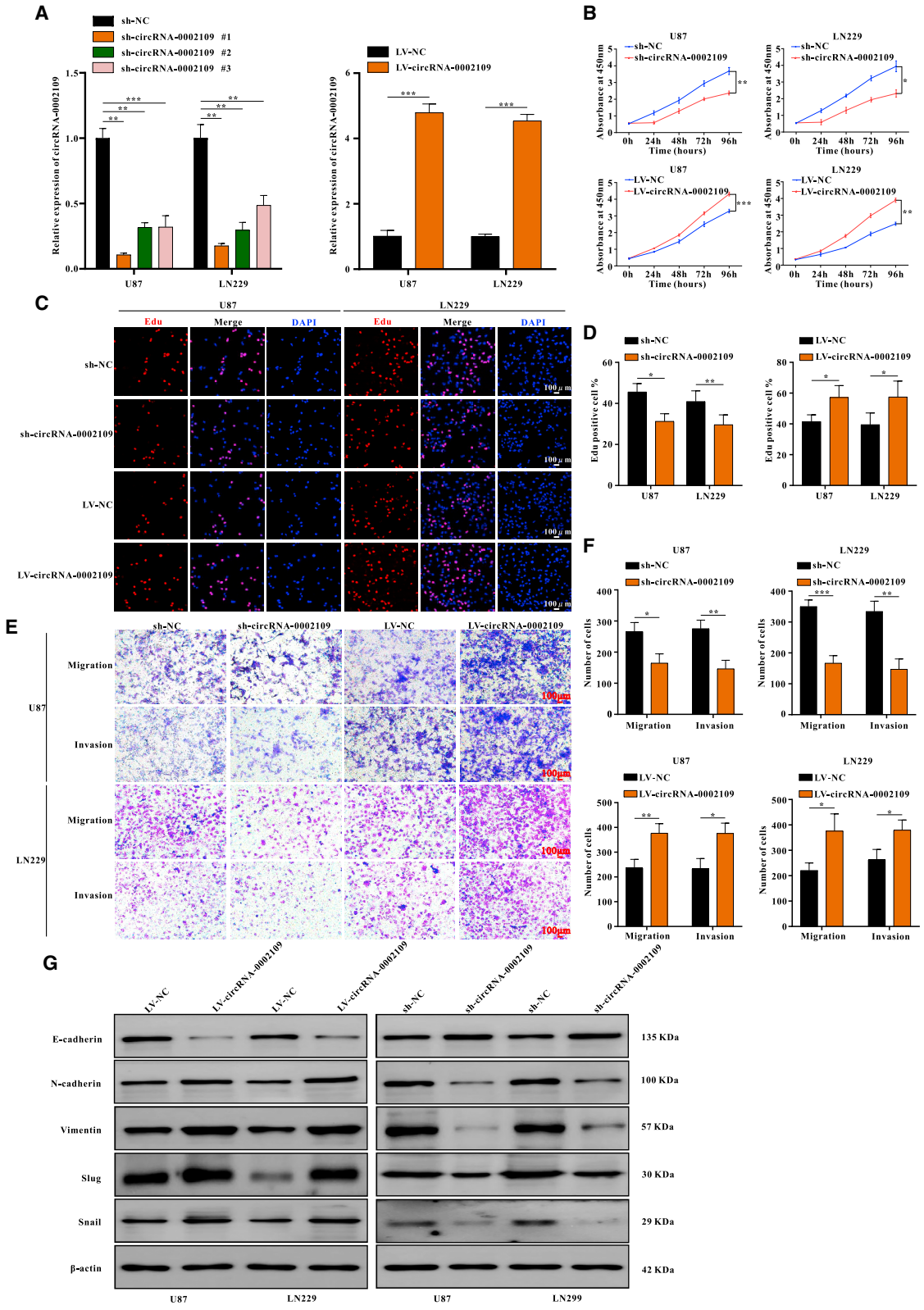
(legend on next page)

analyzed the miRNAs in the GSE103228 dataset (Table S3) and screened 25 downregulated miRNAs with a threshold value of $p < 0.05$ and |log2fold-change| greater than 0.58. The heatmap and volcano map show the differential expression of these miRNAs (Figures 3A and 3B). The miRanda database suggested that miR-129-5P and circRNA-0002109 could bind to each other, with a binding force of 166, and a total free energy of −27.69. In addition, since previous studies have shown that miR-129-5P can play a role in cancer inhibition,[26–28] we chose miR-129-5P as the focus of our study. RT-qPCR analysis was performed on tumor tissues and corresponding adjacent normal tissues, which showed that miR-129-5P was expressed at lower levels in tumor tissues (Figure 3C). RT-qPCR detection in glioma cells also confirmed this conclusion (Figure 3D).

To clarify whether circRNA-0002109 functions as a sponge of miR-129-5P in glioma cells, we conducted an Argonaute2-RNA immunoprecipitation (AGO2-RIP) experiment and confirmed that anti-AGO2 enriched more circRNA-0002109 and miR-129-5P than did anti-immunoglobulin (Ig) G (Figure 7B). Next, we cloned the wild-type circRNA-0002109 and a mutant with a disrupted miR-129-5P binding site into a luciferase vector, and found that the luciferase activity of cells expressing wild-type circRNA-0002109 and transfected with miR-129-5P mimics was significantly lower than that in cells expressing the mutant circRNA-0002109 after miR-129-5P mimic transfection (Figure 3E). Moreover, abundant miR-129-5P was detected by RNA pull-down assay (Figure 3F). Consistent with these results, FISH assays confirmed the colocalization of circRNA-0002109 and miR-129-5P in the cytoplasm of glioma cell lines (Figure S1B). In addition, we found that the expression level of miR-129-5P increased after circRNA-0002109 was knocked down in glioma cells (Figure 3G). These results suggested that circRNA-0002109 inhibited the expression of miR-129-5P by sponging miR-129-5P.

Elevated miR-129-5P expression inhibits the malignant phenotype of glioma cells

To further investigate the potential role of miR-129-5P, we transfected miR-129-5P mimics or inhibitors into U87 and LN229 cells (Figure 4A). Then, we conducted CCK-8 assays and EdU staining, which revealed that overexpression of miR-129-5P inhibits glioma cell proliferation, whereas downregulation of miR-129-5P promotes cell proliferation (Figures 4B and 4C). The transwell assay results showed that the migration and invasion of glioma cells were significantly attenuated after miR-129-5P overexpression, while downregulation of miR-129-5P enhanced these activities (Figure 4D). In conclusion, miR-129-5P acts as a tumor suppressor gene in glioma cells.

miR-129-5P reversed the tumor-promoting effects of circRNA-0002109 in glioma cells

To further clarify whether circRNA-0002109 promotes glioma cell proliferation, migration, and invasion by acting on miR-129-5P, we co-transfected sh-circRNA-0002109 and miR-129-5P inhibitors into U87 and LN229 cells, and rescue experiments showed that inhibition of miR-129-5P expression could partially reverse the effect of sh-circRNA-0002109 (Figure 5A). CCK-8 and EdU staining assays suggested that inhibiting miR-129-5P expression could enhance proliferation. Notably, inhibition of miR-129-5P reversed the decline in proliferation caused by sh-circRNA-0002109 (Figures 5B and 5C). Transwell assays also showed that the miR-129-5P inhibitor reversed the decrease in migration and invasion caused by sh-circRNA-0002109 (Figure 5D). Taken together, these results indicated that circRNA-0002109 promotes the development of glioma cells by inhibiting the antitumor effect of miR-129-5P.

miR-129-5P directly targets the oncogene EMP2

To identify mRNAs with miRNA response elements (MREs) that can bind to miR-129-5P, we predicted the possible downstream target genes of miR-129-5P through the miRanda, miRDB, miRTar-Base, and miRcode databases,[29–32] and obtained 143 genes that were common among all four databases (Figure 6A; Tables S4, S5, S6, S7, and S8). Then, we intersected the 143 genes with the mRNAs upregulated in glioma tissues based on the GSE104267 microarray analysis (Figures S2A and S2B; Table S9), and eight genes were finally identified (Figure 6B). Next, we conducted RT-qPCR experiments on these eight genes in normal human astrocyte (NHA), U87, and LN229 cells, and found that only EMP2 was simultaneously increased in U87 and LN229 cells; its expression was the most abundant compared with the other seven genes investigated (Figures 6C and S2C). RT-qPCR and immunohistochemistry (IHC) showed that EMP2 was highly expressed in glioma tissues (Figures 6D and 6E). Furthermore, we have analyzed the expression of EMP2 in different grades of gliomas based on the Chinese Glioma Genome Atlas (CGGA) databases and The Cancer Genome Atlas (TCGA) databases and discovered that EMP2 expression level was higher in high-grade gliomas than in low-grade glioma, especially in grade IV. Besides, EMP2 expression level was higher in recurrent gliomas than in primary gliomas. In addition, we also performed Kaplan-Meier survival analysis of survival percentage based on TCGA and CGGA data. The results demonstrated that glioma patients with higher EMP2 expression obtained shorter median survival time and poor prognosis compared with the patients with lower expression (Figures S3A–S3D). We have analyzed the expression of EMP2 in these four subtypes by detecting the data from TCGA database and we can see that the expression levels of EMP2 are different in each subtype of glioblastoma; the EMP2 expression level is

Figure 2. High expression of circRNA-0002109 promotes the proliferation, migration, and invasion of glioma cells
(A) RT-qPCR analysis of circRNA-0002109 expression levels after treatment with three sh-RNAs and LV-RNAs. (B–D) CCK-8 assay and EdU staining were performed to assess proliferation ability of cells transduced with sh-circRNA-0002109 or LV-circRNA-0002109. Scale bars, 100 μm. The sampling day of EdU staining is 36 h after the cells adhere to the plates. (E and F) The migration and invasion ability of U87 and LN229 cells were confirmed by transwell assay. Scale bars, 100 μm. (G) Expression level of EMT-related proteins was detected by western blot analysis. Data are presented as mean ± SD of three independent experiments. *$p < 0.05$; **$p < 0.01$; ***$p < 0.001$.
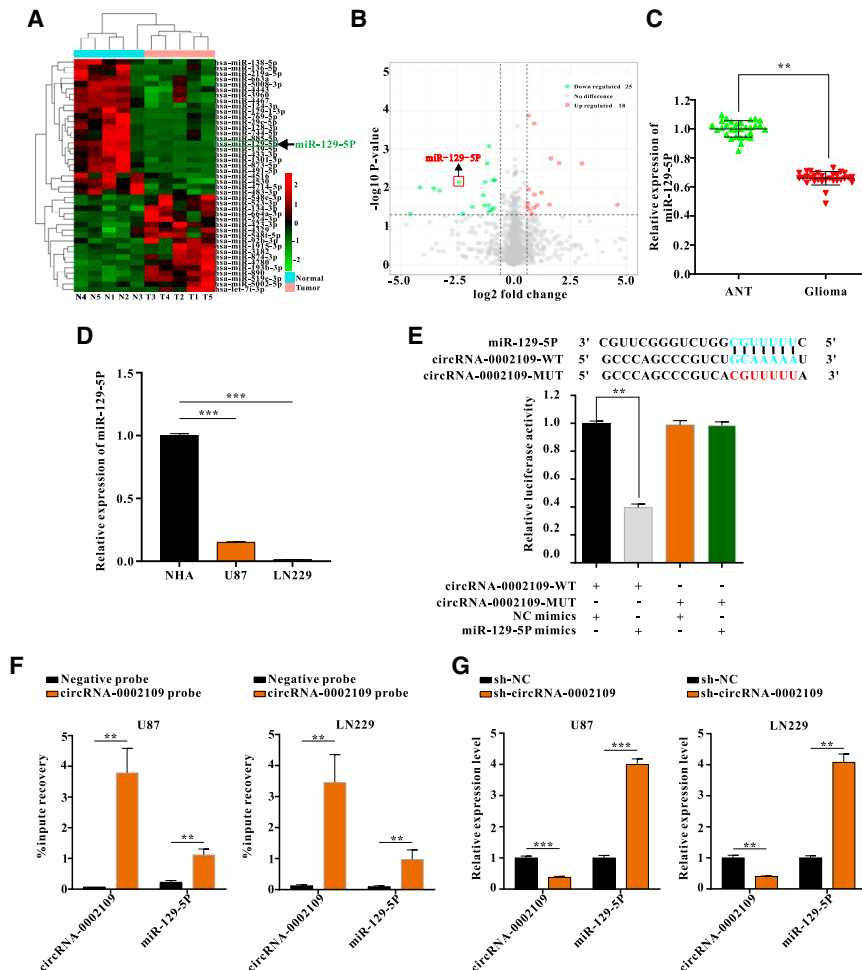
Figure 3. circRNA-0002109 functions as a sponge for miR-129-5P in glioma cells

(A) Heatmap and (B) volcano map of differentially expressed miRNAs between glioma tissues and ANT in GSE103228 microarray. (C) The expression level of miR-129-5P in glioma tissues (n = 30) and (D) cell lines via RT-qPCR analysis. (E) A dual-luciferase reporter assay to determine the direct binding between circRNA-0002109 and miR-129-5P. (F) RNA pull-down assay was performed to verify the enrichment of miR-129-5P by circRNA-0002109 in glioma cells. (G) Expression levels of circRNA-0002109 and miR-129-5P in U87 and LN229 cells transduced with sh-circRNA-0002109 were evaluated by RT-qPCR. Data are presented as mean ± SD of three independent experiments. **p < 0.01; ***p < 0.001.

vasion of glioma cells. Notably, we found that overexpression of EMP2 significantly reversed the inhibitory effects of miR-129-5P mimics on glioma cell proliferation, migration, and invasion (Figures 6I–6K). In conclusion, these findings suggested that EMP2 is an oncogene and a direct target of miR-129-5P in glioma cells.

CircRNA-0002109 facilitates the malignant phenotype of glioma cells by targeting EMP2

To further investigate whether circRNA-0002109 promotes the malignant progression of glioma cells by regulating the downstream target gene EMP2, sh-circRNA-0002109 and EMP2 overexpressing lentiviral vector were co-transduced into U87 and LN229 cells. RT-qPCR analysis showed that sh-circRNA-0002109 could downregulate the expression of EMP2 (Figure 7A). In addition, we conducted an AGO2-RIP experiment, which showed that anti-AGO2 simultaneously enriched more circRNA-0002109 and EMP2 than did anti-IgG (Figure 7B). Next, CCK-8 and EdU staining analysis indicated that overexpression of EMP2 inhibited the decrease in cell proliferation decrease induced by sh-circRNA-0002109 (Figures 7C and 7D). Besides, transwell assays confirmed that overexpression of EMP2 reversed the reduction in migration and invasion caused by circRNA-0002109 knockdown (Figure 7E). In addition, we detected protein changes in EMT marker genes via western blotting and showed that downregulation of circRNA-0002109 inhibited the expression of N-cadherin, Vimentin, Slug, and Snail while enhancing the expression of E-cadherin. It is worth noting that overexpression of EMP2 reverses these changes (Figure 7F). On the other hand, western blotting also demonstrated that inhibition of miR-129-5P expression reversed the downregulation of EMP2 caused by circRNA-0002109 knockdown, whereas overexpression of miR-129-5P reserved the upregulation of EMP2 caused by LV-circRNA-0002109 (Figure 7G). Next, correlation analysis revealed

significantly highest in mesenchymal subtype compared with another three subtypes, so EMP2 can be used as a marker of molecular subtypes in GBM (Figure S3E). These results suggested that the expression level of EMP2 was closely related to glioma progression. Therefore, we focused on EMP2 as the downstream mRNA in our study. To verify that miR-129-5P interacts directly with EMP2, we constructed luciferase reporter plasmids with the wild-type 3′ UTR of EMP2 mRNA and mutant 3′ UTR with a mutated miR-129-5P binding site. The results showed that miR-129-5P mimics significantly reduced the luciferase activity in cells with the wild-type 3′ UTR, while the luciferase activity in cells with the mutant 3′ UTR did not significantly change, indicating that miR-129-5P inhibited the expression of EMP2 by directly binding to the 3′ UTR of EMP2 mRNA (Figure 6F). In addition, in U87 and LN229 cells, miR-129-5P mimics significantly decreased the mRNA and protein expression of EMP2, while miR-129-5P inhibitor significantly increased this expression (Figures 6G and 6H).

Next, we investigated the functions of EMP2 in glioma cells. Overexpression of EMP2 promotes the proliferation, migration, and in-
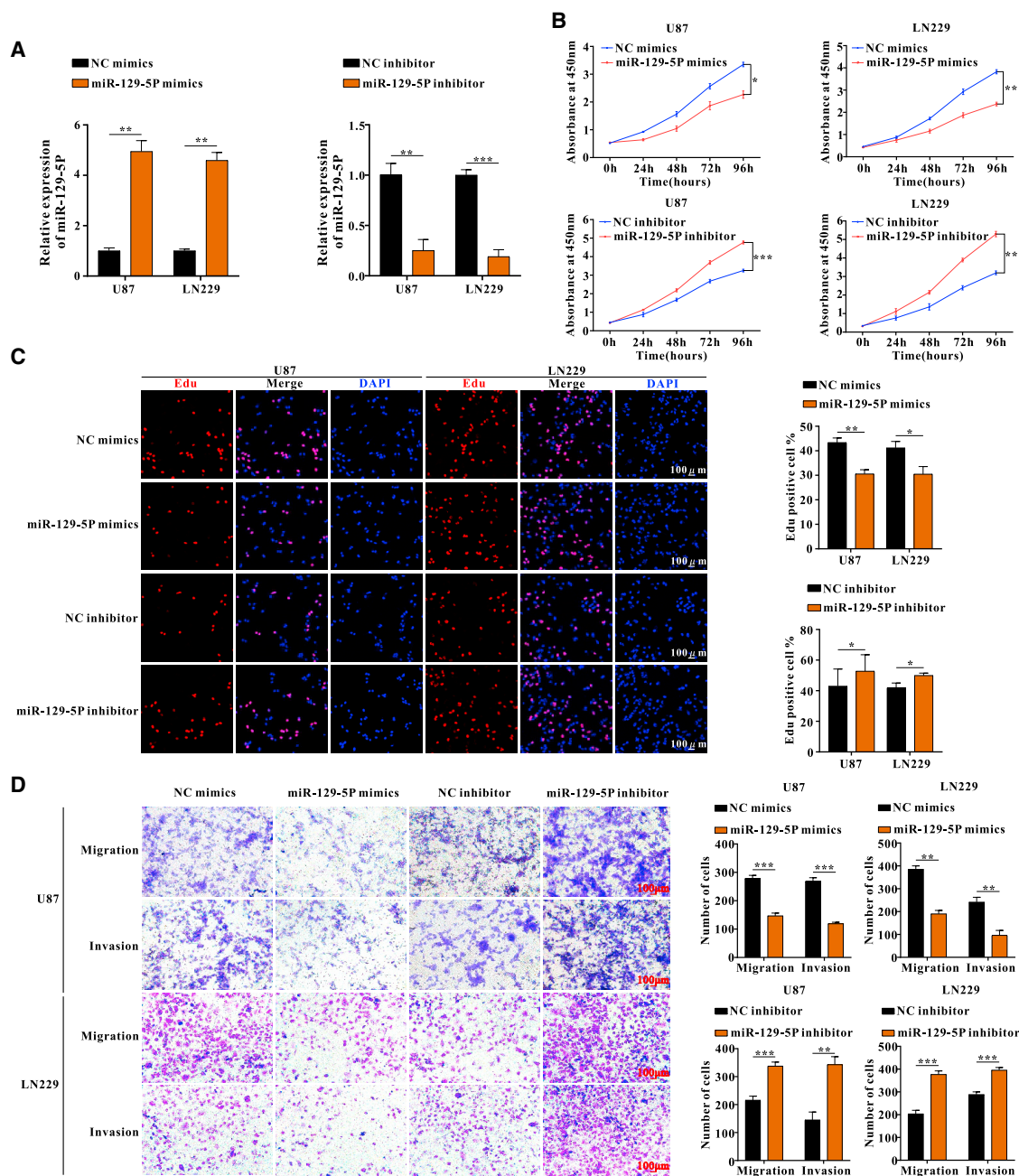
Figure 4. Elevated miR-129-5P expression inhibits the malignant phenotype of glioma cells

(A) The expression levels of miR-129-5P was determined by RT-qPCR in glioma cells transfected with miR-129-5P mimics or miR-129-5P inhibitor. (B) CCK-8 assay and (C) EdU staining were performed to detect the cell proliferation ability. Scale bars, 100 μm. The sampling day of EdU staining is 36 h after the cells adhere to the plates. (D) Effect of miR-129-5P on the migration and invasion of glioma cells was assessed by transwell assay. Scale bars, 100 μm. Data are presented as mean ± SD of three independent experiments. *p < 0.05; **p < 0.01; ***p < 0.001.

that the expression of EMP2 was positively correlated with circRNA-0002109, but negatively correlated with miR-129-5P (Figure 7H). These results indicated that circRNA-0002109 promoted the malignant progression of glioma cells by specifically upregulating of EMP2 expression.

Silencing circRNA-0002109 inhibited xenograft tumor growth *in vivo*

To investigate the regulatory effect of circRNA-0002109 on tumor growth *in vivo*, U87 cells stably transduced with the lentiviral plasmid sh-circRNA-0002109 or LV-EMP2 were subcutaneously injected into
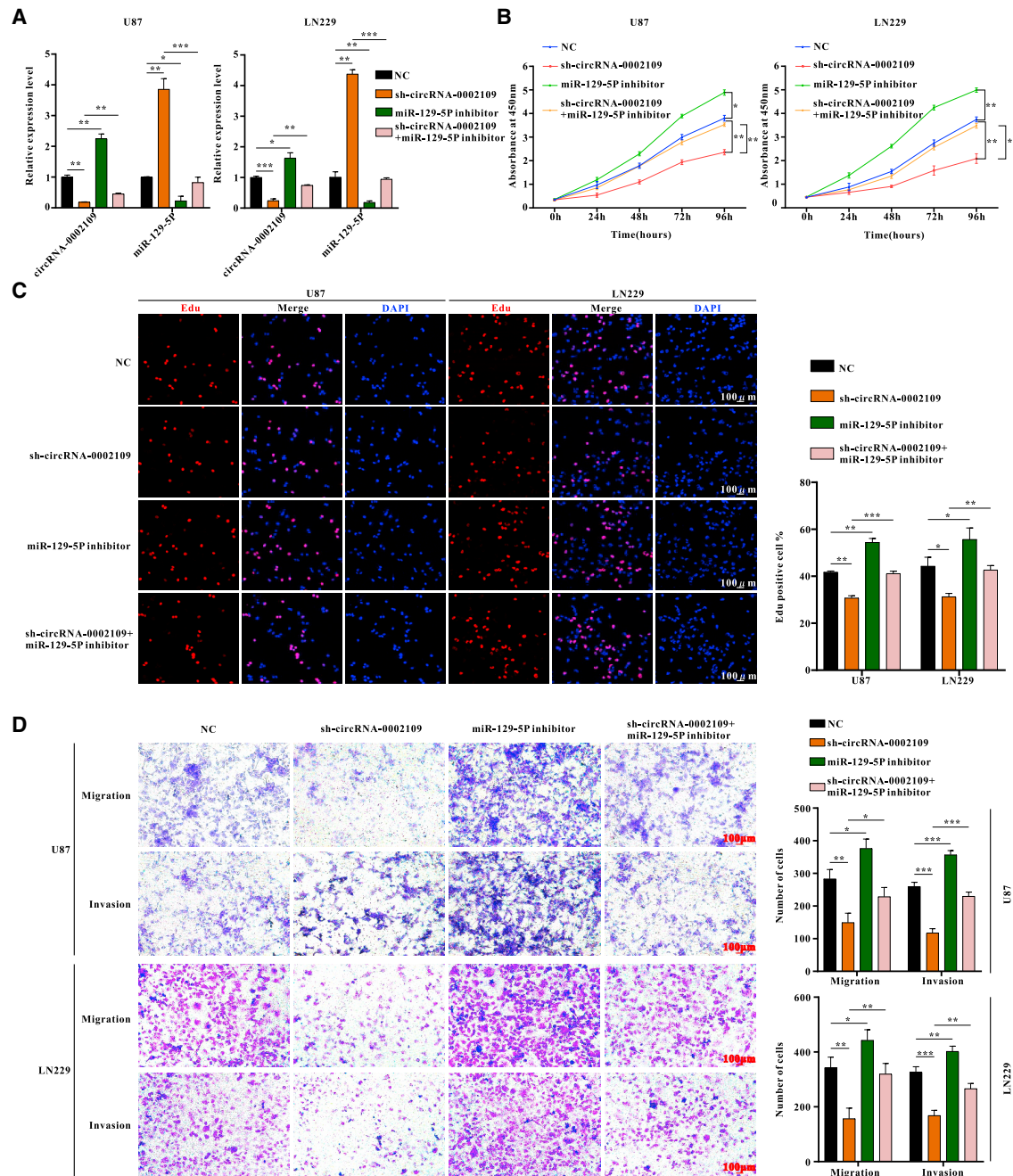
Figure 5. miR-129-5P reversed the tumor-promoting effects of circRNA-0002109 in glioma cells

(A) CircRNA-0002109 and miR-129-5P expression levels were detected by RT-qPCR in glioma cells transduced with sh-circRNA-0002109 or co-transfected with sh-circRNA-0002109 and miR-129-5P inhibitor. Effects of sh-circRNA-0002109 and miR-129-5P inhibitor on the proliferation of U87 and LN229 cells were evaluated by (B) CCK-8 assay and (C) EdU staining. Scale bars, 100 μm. The sampling day of EdU staining is 36 h after the cells adhere to the plates. (D) Transwell assay was performed to evaluate glioma cells' ability of migration and invasion. Scale bars, 100 μm. Data are presented as mean ± SD of three independent experiments. *p < 0.05; **p < 0.01; ***p < 0.001.

nude mice to establish a xenograft tumor model. We observed that knocking down circRNA-0002109 resulted in a significantly smaller xenograft volume and lower weight than those in the control group (sh-NC), and this effect was reversed by transducing cells with LV-EMP2 (Figures 8A–8C). Then, we extracted RNA from the tumors and performed RT-qPCR analysis, which showed that the expression
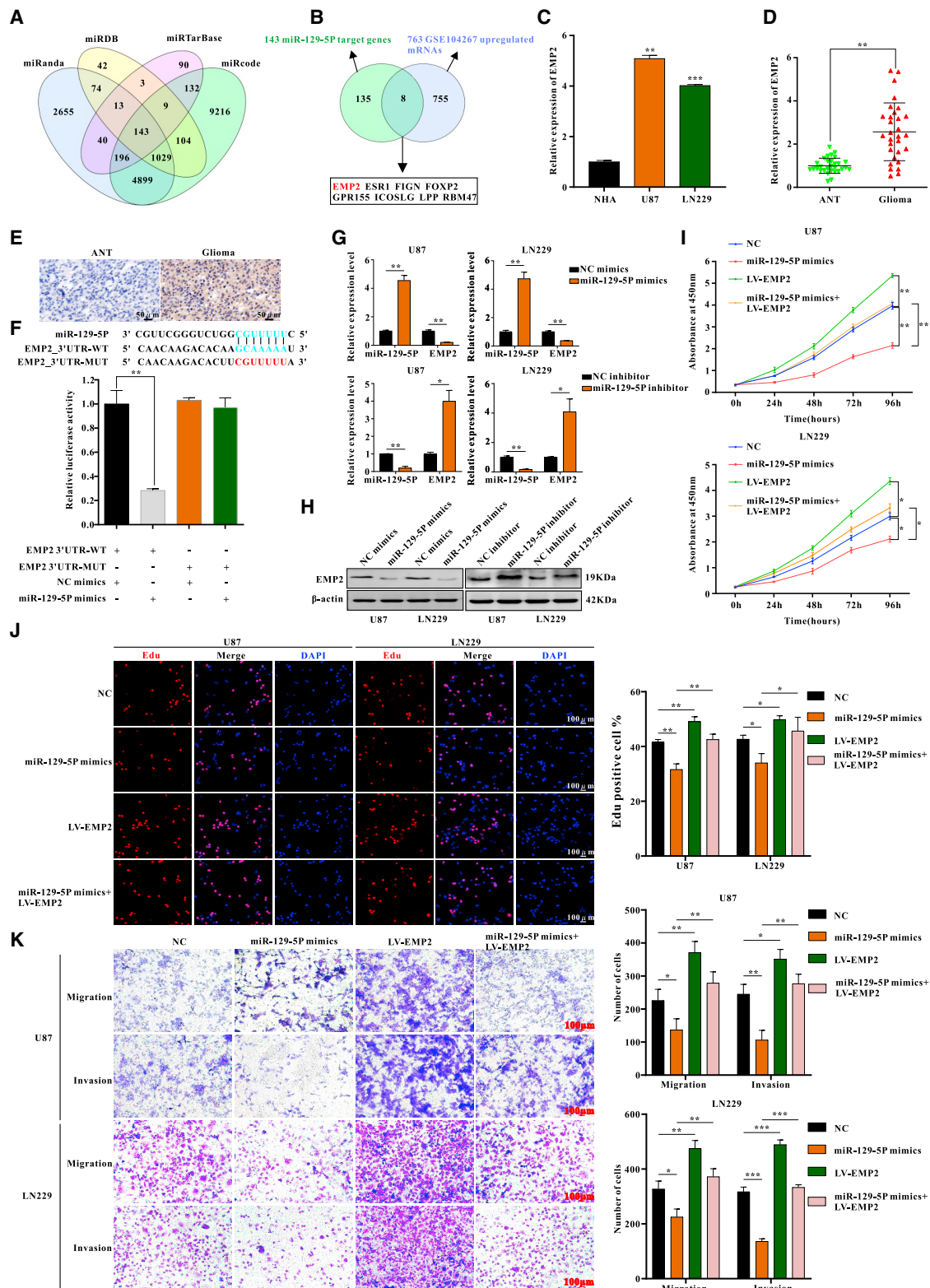
(legend on next page)

of circRNA-0002109 and EMP2 was decreased, while that of miR-129-5P was increased in the tumor tissues (Figure 8D). Furthermore, the IHC staining results showed that, in sh-circRNA-0002109 tumor tissues, EMP2 expression levels were decreased; the expression of EMT markers such as N-cadherin, Vimentin, Slug, and Snail was decreased; and E-cadherin expression levels increased (Figure 8E). These results revealed that knockdown of circRNA-0002109 attenuated the mesenchymal phenotype and confirmed that circRNA-0002109 promotes the malignant progression of glioma *in vivo*.

DISCUSSION

Surgery, chemoradiotherapy, immunotherapy, and related combination therapies can improve the survival prognosis of patients with glioma[33–35]; however, a high recurrence rate remains the major cause of glioma-related death.[36] Therefore, we urgently need to find new targets for the treatment of glioma. In recent years, the regulatory role of circRNAs in various diseases has been confirmed,[37] especially with regard to the occurrence and development of malignant tumors.[38,39] Currently, several circRNAs have been confirmed to play vital roles in the progression of glioma, such as CircNT5E, CircSCAF11, and CircU2AF1.[40–42] In this study, we discovered a new circRNA, named circRNA-0002109, via analysis of the GSE109569 chip, and verified that it is highly expressed in glioma tissues and cells. Mechanistic studies demonstrated that circRNA-0002109 bound to miR-129-5P and attenuated the inhibitory effect of miR-129-5P on its target gene EMP2, leading to EMP2 accumulation and the consequent increases in the proliferation, migration, and invasion of glioma cells.

circRNA-0002109 is generated by reverse splicing exons 4 and 5 of MCM10, a familiar oncogene, and was confirmed by Sanger sequencing. We found that circRNA-0002109 expression was upregulated in glioma tissues and a variety of glioma cell lines. Loss-of-function experiments showed that knockdown of circRNA-0002109 could inhibit glioma cell proliferation, migration, and invasion. These findings suggest that circRNA-0002109 acts as an oncogene to promote a malignant phenotype of glioma.

A large number of studies have shown that circRNAs can competitively bind miRNAs to inhibit their activity, bind RNA-binding proteins to regulate downstream target genes, and translate proteins to promote biological functions.[43,44] In this study, we found that circRNA-0002109 was mainly localized to the cytoplasm, suggesting it exerts a sponging effect on miRNAs. We selected miR-129-5P as the target miRNA based on bioinformatics analysis of the GSE103228

chip. miR-129-5P has been reported to have inhibitory effects on laryngeal cancer, neuroendocrine tumors, and prostate cancer.[26–28] Moreover, we demonstrated that the expression of miR-129-5P in glioma tissues was lower than that in matched tumor-adjacent tissues. Further functional analysis showed that overexpression of miR-129-5P inhibited glioma cell proliferation, migration, and invasion, while the miR-129-5P inhibitor promoted these activities. The binding of circRNA-0002109 to miR-129-5P was confirmed by dual-luciferase reporter, RNA immunoprecipitation (RIP), and pull-down assays. These results suggested that circRNA-0002109 sponged miR-129-5P to exert a tumor-promoting role in glioma cells.

EMP2 is an oncogene that has been studied in many kinds of tumors.[21,22] In 2017, Madhuri Wadehra et al. showed that EMP2 can promote the pathological progression of glioma and is a promising therapeutic target.[24] Besides, Kaplan-Meier survival analysis based on TCGA and CGGA data demonstrated that glioma patients with higher EMP2 expression obtained shorter median survival time and poor prognosis compared with the patients with lower expression. In our study, EMP2 expression was upregulated in glioma tissues, and overexpression of EMP2 greatly promotes the proliferation, migration, and invasion of glioma cells. Upon review of multiple database, we found that EMP2 is a downstream target gene of miR-129-5P and confirmed this association with the dual-luciferase reporter assay. Further experiments indicated that the primary activity of circRNA-0002109 is competitively binding miR-129-5P to indirectly regulate EMP2 expression. Functional analysis showed that circRNA-0002109 promoted the malignant phenotype of glioma cells by upregulating EMP2. A large number of studies has shown that the migration and invasion activities of tumor cells are closely related to EMT.[45,46] Our data revealed that the expression levels of circRNA-0002109 or EMP2 affect the expression levels of EMT markers (such as E-cadherin, N-cadherin, Vimentin, Slug, and Snail), indicating that the circRNA-0002109/miR-129-5P/EMP2 axis promotes the migration and invasion of glioma cells by regulating EMT.

Finally, *in vivo* experiments were conducted to further illustrate the regulatory relationship of the circRNA-0002109/miR-129-5P/EMP2 axis on glioma progression. Our study enriched the understanding of the molecular mechanism by which circRNAs affect glioma genesis. In the future, we can focus on the upstream regulatory factors of circRNA-0002109 and potentially develop a noninvasive method for detecting circRNA-0002109, which is of great significance for the clinical translation of glioma research.

Figure 6. miR-129-5P directly targets the oncogene EMP2
(A) Potential target genes of miR-129-5P predicted by miRanda, miRDB, miRTarBase, and miRcode. (B) Integrated analysis of bioinformatics-predicted target genes and GSE104267 chip was performed to screen for miR-129-5P target genes. The expression level of EMP2 was evaluated by RT-qPCR in (C) cell lines and (D) glioma tissues (n = 30). (E) Immunohistochemistry (IHC) showed EMP2 expression level in glioma tissues. Scale bars, 50 μm. (F) Luciferase reporter assay was used to detect luciferase activity after co-transfecting with miR-129-5P mimics and EMP2-WT or EMP2-MUT reporter plasmid. EMP2 expression level was detected by (G) RT-qPCR and (H) western blotting in U87 and LN229 cells after transfecting with miR-129-5P mimics or miR-129-5P inhibitor. (I) CCK-8 assay and (J) EdU staining analysis of the proliferation ability in LV-EMP2 and miR-129-5P mimics co-transfected cells. Scale bars, 100 μm. The sampling day of EdU staining is 36 h after the cells adhere to the plates. (K) Changes in cell migration and invasion capacity were evaluated by transwell assay in cells transduced with LV-EMP2 or co-transfected miR-129-5P mimics. Scale bars, 100 μm. Data are presented as mean ± SD of three independent experiments. *p < 0.05; **p < 0.01; ***p < 0.001.
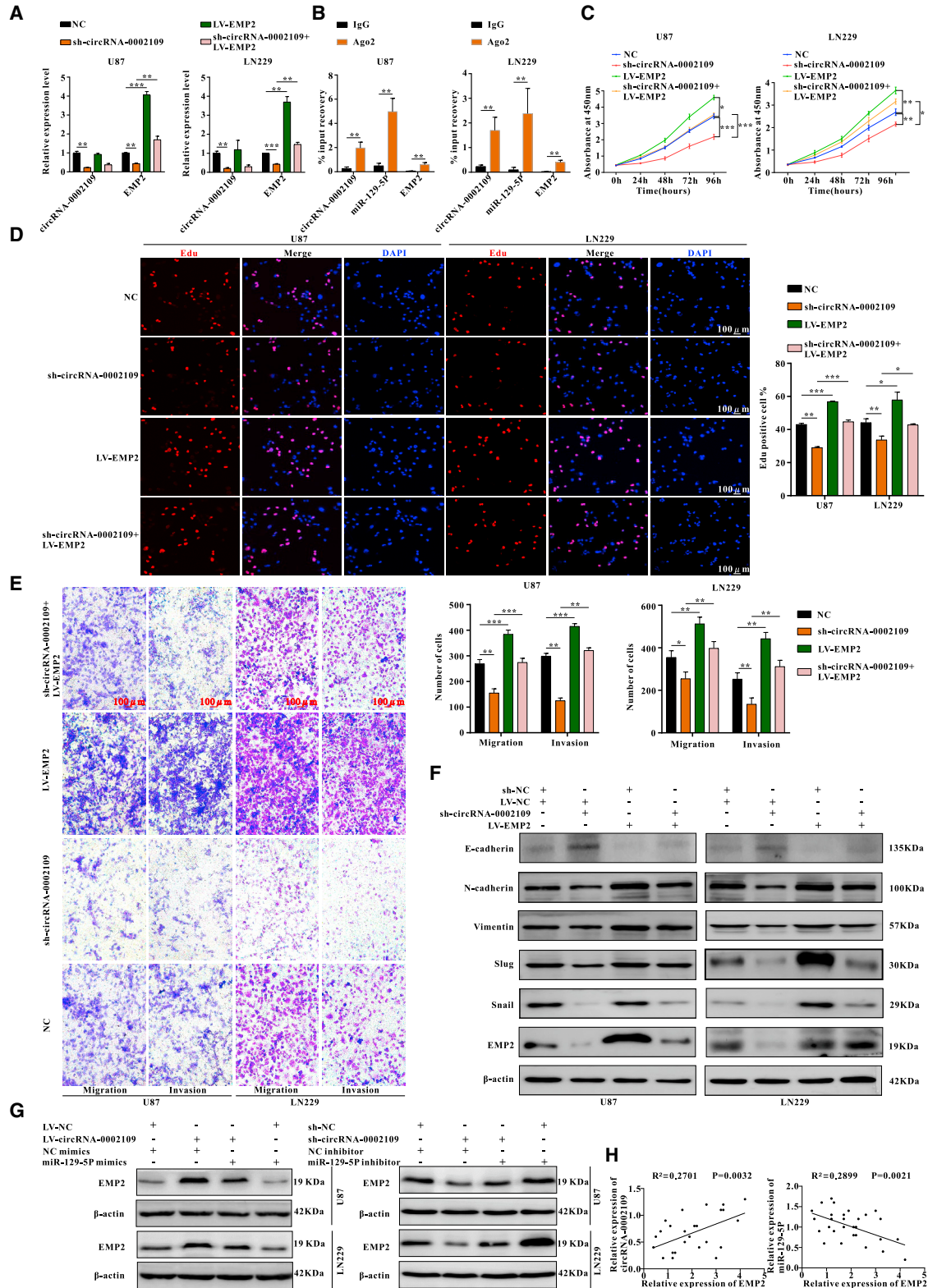
MATERIALS AND METHODS

Glioma tissue samples

In all, 30 pairs of glioma tissues and matched tumor-adjacent tissues were taken from patients who underwent surgical resection at the First Affiliated Hospital of Gannan Medical University. All specimens were immediately frozen in liquid nitrogen after resection and then stored at $-80°C$ prior to use for RT-qPCR analysis. In this study, informed consent was obtained from each patient, and the project protocol was approved by the ethics committee of the First Affiliated Hospital of Gannan Medical University.

Cell lines and cell culture

Human glioma cell lines (U87, LN229, U251, SHG44, A172) and a normal astrocyte cell line (NHA) were purchased from the Cell Bank of the Chinese Academy of Sciences (Shanghai, China), identified, and tested for mycoplasma contamination. Cells were routinely cultured in Dulbecco's modified Eagle's medium (DMEM, Invitrogen) supplemented with 10% (v/v) fetal bovine serum (FBS, HyClone, Logan, UT), penicillin (200 units/mL), and streptomycin (100 μg/mL) and cultured at $37°C$ in a 5% CO_2 humidified air incubator (Thermo Scientific, Waltham, MA).

RNA isolation, RNase R digestion, and RT-qPCR

Total RNA from tissues or cells was extracted with TRIzol Reagent (Invitrogen, United States) based on the manufacturer's protocol. RNA from the nuclei and cytoplasm of cell lines was extracted using a Nuclear/Cytosol Fractionation Kit (BioVision, United States). For RNase R digestion, 5 μg of total RNA was incubated for 10 min at $37°C$ in the presence or absence of 4 U/μg RNase R (Geneseed Biotech, Guangzhou, China). To quantify circRNA, mRNA and miRNA, RT-qPCR samples were prepared with GoTap qPCR Master Mix (Promega, United States) and run on a 7500 Fast Real-time PCR System (Applied Biosystem, Foster City, CA). GAPDH and U6 were used as the internal reference genes, and the relative expression was calculated using the $2^{-\triangle\triangle Ct}$ method. The PCR primers used are listed in Table S10.

Western blot analysis

Total protein was extracted from the cells using radio-immunoprecipitation assay lysis buffer. A bicinchoninic acid (BCA) protein assay kit (Thermo, United States) was used to measure the protein concentration. Equal amounts of protein were separated by SDS-PAGE through gels and then transferred onto polyvinylidene fluoride (PVDF) membranes (Bio-Rad, United States) in accordance with the standard procedure. The membranes were blocked with 5% skim milk at room temperature for 2 h before they were incubated with primary antibody at $4°C$ overnight. Subsequently, the secondary antibody was incubated at room temperature for 1 h the next day and the protein bands were visualized by chemiluminescence and imaged. Information on the antibodies used is listed in Table S11.

Cell transduction/transfection

Lentiviral vectors (control small hairpin RNA [sh-RNA] lentiviral vectors, circRNA-0002109 sh-RNA lentiviral vectors, control lentiviral activation vectors, circRNA-0002109 lentiviral activation vectors, EMP2 lentiviral activation vectors) were purchased from GeneChem (Shanghai, China) and were transduced into cells according to the manufacturer's instructions. In brief, glioma cells were seeded in a six-well plate and cultured overnight in complete medium to a confluency of 50%. The original medium was replaced with 1mL of OPTI-MEM (Invitrogen, United States) and polybrene (5 μg/mL, GeneChem, Shanghai, China) containing the lentiviral particles (multiplicity of infection [MOI] of 10) to transduce the cells. The transduced cells were cultured in the presence of 2.0 μg/mL puromycin for 2 weeks to select stable transduced cells. The virus titers of sh-circRNA-0002109, LV-circRNA-0002109, and LV-EMP2 are 3.5E+8TU/mL, 7E+8TU/mL and 3.5E+8TU/mL, respectively. miR-129-5P mimics/inhibitor and NC mimics/inhibitor were purchased from RiboBio (Guangzhou, China) and transfected into cells according to the manufacturer's instructions. The effective sequences of lentiviral vector and the sequence of miRNA mimics/inhibitor shown in Tables S12 and S13.

CCK-8 assay

The proliferation of U87 and LN229 cells was measured with a CCK-8 kit (Dojindo, Shanghai, China). Twenty-four hours after transfection, the cells were seeded into 96-well plates at approximately 1,000 cells per well and incubated for 0, 24, 48, 72, or 96 h. CCK-8 reagent was added to DMEM to produce the working solution at a ratio of 1:10, and then 100μL of this solution was added per well and incubated at $37°C$ for 2 h. We calculated the absorbance of the solution at 450 nm on a microplate reader.

EdU assay

An EdU kit (Life Technologies Corporation, Carlsbad, CA) was used to assess cell proliferation. Glioma cell lines were cultured in 96-well plates, and EdU experiments performed after the cells adhered to the plate bottom for 36 h. According to the manufacturer's instructions, cells were treated with 10 μM EdU reagent at $37°C$ for 2 h before they were fixed with formaldehyde for 30 min. A Click-iT EdU kit was used to detect EdU levels at room temperature. After Hoechst

Figure 7. circRNA-0002109 facilitates the malignant phenotype of glioma cells by targeting EMP2

(A) RT-qPCR analysis for EMP2 expression level after transducing sh-circRNA-0002109 or co-transducing LV-EMP2. (B) Ago2-RIP assay was performed to analysis the enrichment of circRNA-0002109, miR-129-5P, and EMP2. Cell proliferation was determined by (C) CCK-8 assay and (D) EdU staining in glioma cells after transducing with sh-circRNA-0002109 or co-transfected with sh-circRNA-0002109 and EMP2 overexpressed lentivirus plasmids. Scale bars, 100 μm. The sampling day of EdU staining is 36 h after the cells adhere to the plates. (E) Effects of sh-circRNA-0002109 and LV-EMP2 on the migration and invasion of U87 and LN229 cells were determined by transwell assay. Scale bars, 100 μm. (F) EMT-related proteins expression levels in U87 and LN229 cells with knockdown of circRNA-0002109 and overexpression of EMP2. (G) Protein levels of EMP2 in U87 and LN229 cells transfected with different treatments by western blotting. (H) The correlation of EMP2/miR-129-5P and EMP2/circRNA-0002109 in glioma tissues (n = 30) was analyzed by RT-qPCR. Data are presented as mean ± SD of three independent experiments. *p < 0.05; **p < 0.01; ***p < 0.001.
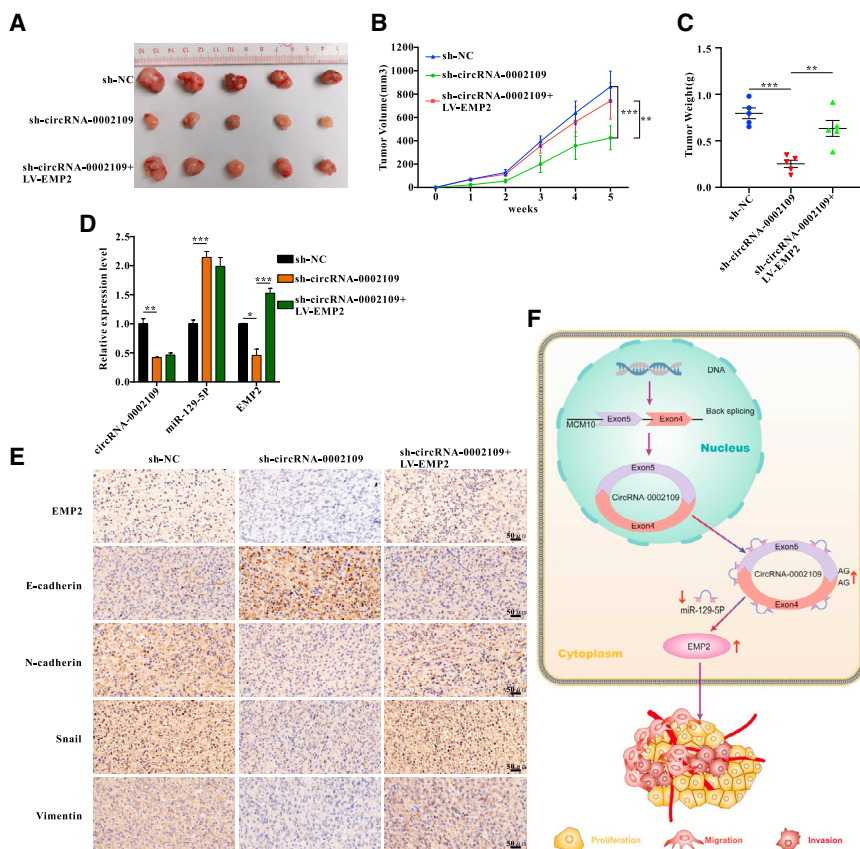
Figure 8. Silencing circRNA-0002109 inhibited xenograft tumor growth *in vivo*

(A) Photographs of tumors that developed in the xenograft-transplanted nude mice tumor models after cell injection of U87-sh-circRNA-0002109 or co-transduced with sh-circRNA-0002109 and LV-EMP2 at 5 weeks. (B) Growth curve of sh-circRNA-0002109 or co-transduced with sh-circRNA-0002109 and LV-EMP2 cell-derived subcutaneous tumor xenografts. (C) Weight of tumor xenografts originated from sh-circRNA-0002109 group or co-transduced with sh-circRNA-0002109 and LV-EMP2 cells group at 5 weeks. (D) Relative expression levels of circRNA-0002109, miR-129-5P, and EMP2 in sh-circRNA-0002109 or co-transduced with sh-circRNA-0002109 and LV-EMP2 cell-derived tumor xenografts. (E) Changes of EMP2, E-cadherin, N-cadherin, Snail, and Vimentin expression level in xenograft tumors were detected by IHC staining. Scale bars, 50 μm. (F) Schematic diagram shows that circRNA-0002109 promotes glioma malignant progression through regulating the miR-129-5P/EMP2 axis.

ufacturer's instructions. The nuclei were stained with DAPI and observed under a fluorescence microscope (Olympus, Tokyo, Japan). Image-Pro Plus 6.0 software (Media Cybernetics, Rockville, MD) was used to analyze the images.

Luciferase reporter assay

The circRNA-0002109 and EMP2 sequences and their corresponding mutants were synthesized and inserted into the psi-CHECK2 vector (Promega, WI). These luciferase reporter plasmids were co-transfected with miR-129-5P mimics or NC mimics into HEK293T cells for 48 h and then the luciferase activity was detected using the Dual-Luciferase Reporter Assay System (Promega E1910) on a Cytation 3 Imaging reader (BioTek). Finally, the relative luciferase activity was calculated.

RIP

We purchased an EZMagna RIP kit (Millipore, United States) and used it according to the manufacturer's instructions. Briefly, U87 and LN229 cells were lysed, and the collected lysates were incubated with magnetic beads bound to human Argonaute2 (AGO2) or normal control IgG antibody. The magnetic beads were incubated with proteinase K to eliminate any bound protein. Finally, immunoprecipitated RNA was extracted, purified, and detected by RT-qPCR.

Pull-down assay

Biotin-circRNA-0002109 and biotin-NC probes were synthesized. The pull-down experiment was carried out according to the relevant experimental instructions. Briefly, U87 and LN229 cells were lysed and subjected to ultrasonication. The circRNA-0002109 probe and control probe were incubated with cell lysate overnight at 37°C. After hybridization, precleaned magnetic beads were added to the lysate and incubated at 37°C for 1 h to generate circRNA-probe-bead

33342 staining, EdU-positive cells were observed under a fluorescence microscope (Olympus, Tokyo, Japan). Image-Pro Plus 6.0 software (Media Cybernetics, Rockville, MD) was used to calculate the proportion of EdU-positive cells within the total cell population.

Migration and invasion assays

The migration and invasion abilities of glioma cells were evaluated with transwell chambers (Corning Life Sciences, MA). At 24 h after transfection, the cells were pretreated and resuspended in serum-free medium before they were seeded in the upper transwell chamber (approximately 5,000 cells per well), and medium with 10% FBS was added to the lower chamber. After 24 h, the cells on the bottom surface of the upper chamber were fixed with 4% paraformaldehyde for 30 min, stained with 0.1% crystal violet solution for 10 min, and then viewed under a fluorescence microscope. Similar to the transwell migration experiment, the invasion experiment was performed with the upper membrane of the transwell chambers coated with Matrigel (BD Biosciences, NJ).

FISH

An RNA FISH Kit (Roche Applied Science, Germany) was used to detect the subcellular localization of circRNA-0002109 and the colocalization of circRNA-0002109 with miR-129-5P in glioma cells. The circRNA-0002109 and miR-129-5P FISH probes were synthesized by GenePharma (Shanghai, China) and tested according to the man-

complexes. After the beads were washed with washing buffer, RNA attached to magnetic beads was purified and analyzed by RT-qPCR. The probe sequences are listed in Table S14.

IHC

Tumor specimens were fixed with 4% formaldehyde, dehydrated, paraffin embedded, and sliced. The samples were incubated with primary antibody at 4°C overnight, washed three times, and then incubated with biotinylated secondary antibody (1:500 dilution, Santa Cruz Biotechnology, United States) at room temperature for 2 h the next day. The location of the protein was determined by the avidin biotinylated peroxidase complex.

Xenograft animal assay

To assess the tumorigenicity of circRNA-0002109, we purchased 4-week-old male BALB/c nude mice from the Laboratory Animal Center of Southern Medical University (Guangzhou, China) and housed them under specific pathogen-free (SPF) conditions. U87 cells were transduced with lentivirus, and the nude mice were randomly divided into three groups. After transduction, U87-sh-NC, U87-sh-circRNA-0002109, and U87-sh-circRNA-0002109 + U87-LV-EMP2 cells were subcutaneously injected into the flanks of nude mice. The tumor volume was measured every 7 days after tumor formation. After 5 weeks, the nude mice were killed, the tumors were isolated and weighed, and the final volume was calculated with the following formula: volume = $0.5 \times (\text{length}) \times (\text{width})^2$. All procedures were conducted in accordance with the National Institutes of Health Guide for the Care and Use of Laboratory and were approved by the Animal Experimental Committee of Southern Medical University.

Statistical analysis

SPSS 25.0 software (SPSS, Chicago, IL) and GraphPad Prism 8.0 (GraphPad Software, San Diego, CA) were used for statistical analysis of the data. The differences between groups were analyzed by Student's t -test. Data are presented as the mean ± standard deviation (SD), of three independent experiments. In each technical replicate, we set three biological replicates of each group. A p value less than 0.05 was considered statistically significant.

SUPPLEMENTAL INFORMATION

Supplemental information can be found online at https://doi.org/10.1016/j.omtn.2021.11.011.

ACKNOWLEDGMENTS

AUTHOR CONTRIBUTIONS

X.H., L.B., Z.X., and G.H. designed the study. X.H. and L.B. performed most of the experiments with assistance from X.J., C.S., and S.N. X.J. and C.S. conducted computational analysis and data curation from the literature. X.H., L.B., and S.N. wrote the original manuscript. Z.X. helped to revise the manuscript. G.H. and Z.X. supervised the study.

DECLARATION OF INTERESTS

The authors declare no competing interests.

REFERENCES

1. Lapointe, S., Perry, A., and Butowski, N.A. (2018). Primary brain tumours in adults. Lancet 392, 432–446.

2. Baumert, B.G., Hegi, M.E., van den Bent, M.J., von Deimling, A., Gorlia, T., Hoang-Xuan, K., Brandes, A.A., Kantor, G., Taphoorn, M.J.B., Hassel, M.B., et al. (2016). Temozolomide chemotherapy versus radiotherapy in high-risk low-grade glioma (EORTC 22033-26033): a randomised, open-label, phase 3 intergroup study. Lancet Oncol. 17, 1521–1532.

3. Wijnenga, M.M.J., French, P.J., Dubbink, H.J., Dinjens, W.N.M., Atmodimedjo, P.N., Kros, J.M., Smits, M., Gahrmann, R., Rutten, G.J., Verheul, J.B., et al. (2018). The impact of surgery in molecularly defined low-grade glioma: an integrated clinical, radiological, and molecular analysis. Neuro Oncol. 20, 103–112.

4. Louis, D.N., Ohgaki, H., Wiestler, O.D., Cavenee, W.K., Burger, P.C., Jouvet, A., Scheithauer, B.W., and Kleihues, P. (2007). The 2007 WHO classification of tumours of the central nervous system. Acta Neuropathol. 114, 97–109.

5. Chinot, O.L., Wick, W., Mason, W., Henriksson, R., Saran, F., Nishikawa, R., Carpentier, A.F., Xuan, K.H., Kavan, P., Cernea, D., et al. (2014). Bevacizumab plus radiotherapy-temozolomide for newly diagnosed glioblastoma. N. Engl. J. Med. 370, 709–722.

6. Gilbert, M.R., Dignam, J.J., Armstrong, T.S., Wefel, J.S., Blumenthal, D.T., Vogelbaum, M.A., Colman, H., Chakravarti, A., Pugh, S., Won, M., et al. (2014). A randomized trial of bevacizumab for newly diagnosed glioblastoma. N. Engl. J. Med. 370, 699–708.

7. Sanger, H.L., Klotz, G., Riesner, D., Gross, H.J., and Kleinschmidt, A.K. (1976). Viroids are single-stranded covalently closed circular RNA molecules existing as highly base-paired rod-like structures. Proc. Natl. Acad. Sci. U S A 73, 3852–3856.

8. Hsu, M.T., and Coca-Prados, M. (1979). Electron microscopic evidence for the circular form of RNA in the cytoplasm of eukaryotic cells. Nature 280, 339–340.

9. Wang, Y., Liu, J., Ma, J., Sun, T., Zhou, Q., Wang, W., Wang, G., Wu, P., Wang, H., Jiang, L., et al. (2019). Exosomal circRNAs: biogenesis, effect and application in human diseases. Mol. Cancer 18, 116.

10. Kristensen, L.S., Andersen, M.S., Stagsted, L.V.W., Ebbesen, K.K., Hansen, T.B., and Kjems, J. (2019). The biogenesis, biology and characterization of circular RNAs. Nat. Rev. Genet. 20, 675–691.

11. Suzuki, H., and Tsukahara, T. (2014). A view of pre-mRNA splicing from RNase R resistant RNAs. Int. J. Mol. Sci. 15, 9331–9342.

12. Arnaiz, E., Sole, C., Manterola, L., Iparraguirre, L., Otaegui, D., and Lawrie, C.H. (2019). CircRNAs and cancer: biomarkers and master regulators. Semin. Cancer Biol. 58, 90–99.

13. Thomson, D.W., and Dinger, M.E. (2016). Endogenous microRNA sponges: evidence and controversy. Nat. Rev. Genet. 17, 272–283.

14. Hansen, T.B., Jensen, T.I., Clausen, B.H., Bramsen, J.B., Finsen, B., Damgaard, C.K., and Kjems, J. (2013). Natural RNA circles function as efficient microRNA sponges. Nature 495, 384–388.

15. Zhang, M., Huang, N., Yang, X., Luo, J., Yan, S., Xiao, F., Chen, W., Gao, X., Zhao, K., et al. (2018). A novel protein encoded by the circular form of the SHPRH gene suppresses glioma tumorigenesis. Oncogene 37, 1805–1814.

16. Xia, X., Li, X., Li, F., Wu, X., Zhang, M., Zhou, H., Huang, N., Yang, X., Xiao, F., Liu, D., et al. (2019). A novel tumor suppressor protein encoded by circular AKT3 RNA inhibits glioblastoma tumorigenicity by competing with active phosphoinositide-dependent kinase-1. Mol. Cancer 18, 131.

17. Huang, A., Zheng, H., Wu, Z., Chen, M., and Huang, Y. (2020). Circular RNA-protein interactions: functions, mechanisms, and identification. Theranostics 10, 3503–3517.

18. Guo, X., Zhou, Q., Su, D., Luo, Y., Fu, Z., and Huang, L. (2020). Circular RNA circBFAR promotes the progression of pancreatic ductal adenocarcinoma via the miR-34b-5p/MET/Akt axis. Mol. Cancer *19*, 83.

19. Pan, Z., Cai, J., Lin, J., Zhou, H., Peng, J., Liang, J., Xia, L., Yin, Q., Zou, B., Zheng, J., et al. (2020). A novel protein encoded by circFNDC3B inhibits tumor progression and EMT through regulating Snail in colon cancer. Mol. Cancer *19*, 71.

20. Amin, M.K.B.A., Shimizu, A., and Ogita, H. (2019). The pivotal roles of the epithelial membrane protein family in cancer invasiveness and metastasis. Cancers (Basel) *11*, 1620.

21. Dillard, C., Kiyohara, M., Mah, V., McDermott, S.P., Bazzoun, D., Tsui, J., Chan, A.M., Haddad, G., Pellegrini, M., Chang, Y., et al. (2020). EMP2 is a novel regulator of stemness in breast cancer cells. Mol. Cancer Ther. *19*, 1682–1695.

22. Kiyohara, M.H., Dillard, C., Tsui, J., Kim, S.R., Lu, J., Sachdev, D., Goodglick, L., Tong, M., Torous, V.F., Aryasomayajula, C., et al. (2017). EMP2 is a novel therapeutic target for endometrial cancer stem cells. Oncogene *36*, 5793–5807.

23. Chung, L.K., Pelargos, P.E., Chan, A.M., Demos, J.V., Lagman, C., Sheppard, J.P., Nguyen, T., Chang, Y., Hojat, S.A., Prins, R.M., et al. (2018). Tissue microarray analysis for epithelial membrane protein-2 as a novel biomarker for gliomas. Brain Tumor Pathol. *35*, 1–9.

24. Qin, Y., Takahashi, M., Sheets, K., Soto, H., Tsui, J., Pelargos, P., Antonios, J.P., Kasahara, N., Yang, I., Prins, R.M., et al. (2017). Epithelial membrane protein-2 (EMP2) promotes angiogenesis in glioblastoma multiforme. J. Neurooncol. *134*, 29–40.

25. Wang, R., Zhang, S., Chen, X., Li, N., Li, J., Jia, R., Pan, Y., and Liang, H. (2018). EIF4A3-induced circular RNA MMP9 (circMMP9) acts as a sponge of miR-124 and promotes glioblastoma multiforme cell tumorigenesis. Mol. Cancer *17*, 166.

26. Shen, N., Huang, X., and Li, J. (2016). Upregulation of miR-129-5p affects laryngeal cancer cell proliferation, invasiveness, and migration by affecting STAT3 expression. Tumour Biol. *37*, 1789–1796.

27. Dossing, K.B., Binderup, T., Kaczkowski, B., Jacobsen, A., Rossing, M., Winther, O., Federspile, B., Knigge, U., Kjaer, A., and Hansen, L.F. (2014). Down-regulation of miR-129-5p and the let-7 family in neuroendocrine tumors and metastases leads to up-regulation of their targets Egr1, G3bp1, Hmga2 and Bach1. Genes (Basel) *6*, 1–21.

28. Valentino, A., Calarco, A., Di Salle, A., Finicelli, M., Crispi, S., Calogero, R.A., Riccardo, F., Sciarra, A., Gentilucci, A., Galderisi, U., et al. (2017). Deregulation of microRNAs mediated control of carnitine cycle in prostate cancer: molecular basis and pathophysiological consequences. Oncogene *36*, 6030–6040.

29. Chen, Y., and Wang, X. (2020). miRDB: an online database for prediction of functional microRNA targets. Nucleic Acids Res. *48*, D127–D131.

30. Chou, C.H., Shrestha, S., Yang, C.D., Chang, N.W., Lin, Y.L., Liao, K.W., Huang, W.C., Sun, T.H., Tu, S.J., Lee, W.H., et al. (2018). miRTarBase update 2018: a resource for experimentally validated microRNA-target interactions. Nucleic Acids Res. *46*, D296–D302.

31. Jeggari, A., Marks, D.S., and Larsson, E. (2012). miRcode: a map of putative microRNA target sites in the long non-coding transcriptome. Bioinformatics *28*, 2062–2063.

32. Betel, D., Koppal, A., Agius, P., Sander, C., and Leslie, C. (2010). Comprehensive modeling of microRNA targets predicts functional non-conserved and non-canonical sites. Genome Biol. *11*, R90.

33. Stummer, W., Pichlmeier, U., Meinel, T., Wiestler, O.D., Zanella, F., and Reulen, H.-J. (2006). Fluorescence-guided surgery with 5-aminolevulinic acid for resection of malignant glioma: a randomised controlled multicentre phase III trial. Lancet Oncol. *7*, 392–401.

34. Prabhu, R.S., Won, M., Shaw, E.G., Hu, C., Brachman, D.G., Buckner, J.C., Stelzer, K.J., Barger, G.R., Brown, P.D., Gilbert, M.R., et al. (2014). Effect of the addition of chemotherapy to radiotherapy on cognitive function in patients with low-grade glioma: secondary analysis of RTOG 98-02. J. Clin. Oncol. *32*, 535–541.

35. Yang, M., Oh, I.Y., Mahanty, A., Jin, W.L., and Yoo, J.S. (2020). Immunotherapy for glioblastoma: current state, challenges, and future perspectives. Cancers (Basel) *12*, 2334.

36. Xue, J., Zhao, Z., Zhang, L., Xue, L., Shen, S., Wen, Y., Wei, Z., Wang, L., Kong, L., Sun, H., et al. (2017). Neutrophil-mediated anticancer drug delivery for suppression of postoperative malignant glioma recurrence. Nat. Nanotechnol. *12*, 692–700.

37. Yang, Q., Li, F., He, A., and Yang, B.B. (2021). Circular RNAs: expression, localization, and therapeutic potentials. Mol. Ther. *29*, 1683–1702.

38. Wang, S., Zhang, K., Tan, S., Xin, J., Yuan, Q., Xu, H., Xu, X., Liang, Q., Christiani, D.C., Wang, M., et al. (2021). Circular RNAs in body fluids as cancer biomarkers: the new frontier of liquid biopsies. Mol. Cancer *20*, 13.

39. Yang, X., Ye, T., Liu, H., Lv, P., Duan, C., Wu, X., Jiang, K., Lu, H., Xia, D., Peng, E., et al. (2021). Expression profiles, biological functions and clinical significance of circRNAs in bladder cancer. Mol. Cancer *20*, 4.

40. Wang, R., Zhang, S., Chen, X., Li, N., Li, J., Jia, R., Pan, Y., and Liang, H. (2018). CircNT5E acts as a sponge of miR-422a to promote glioblastoma tumorigenesis. Cancer Res. *78*, 4812–4825.

41. Meng, Q., Li, S., Liu, Y., Zhang, S., Jin, J., Zhang, Y., Guo, C., Liu, B., and Sun, Y. (2019). Circular RNA circSCAF11 accelerates the glioma tumorigenesis through the miR-421/SP1/VEGFA axis. Mol. Ther. Nucleic Acids *17*, 669–677.

42. Li, G., Huang, M., Cai, Y., Yang, Y., Sun, X., and Ke, Y. (2019). Circ-U2AF1 promotes human glioma via derepressing neuro-oncological ventral antigen 2 by sponging hsa-miR-7-5p. J. Cell Physiol. *234*, 9144–9155.

43. Salmena, L., Poliseno, L., Tay, Y., Kats, L., and Pandolfi, P.P. (2011). A ceRNA hypothesis: the Rosetta Stone of a hidden RNA language? Cell *146*, 353–358.

44. Saaoud, F., Drummer, I.V.C., Shao, Y., Sun, Y., Lu, Y., Xu, K., Ni, D., Jiang, X., Wang, H., and Yang, X. (2020). Circular RNAs are a novel type of non-coding RNAs in ROS regulation, cardiovascular metabolic inflammations and cancers. Pharmacol. Ther. *220*, 107715.

45. Yang, J., Antin, P., Berx, G., Blanpain, C., Brabletz, T., Bronner, M., Campbell, K., Cano, A., Casanova, J., Christofori, G., et al. (2020). Guidelines and definitions for research on epithelial-mesenchymal transition. Nat. Rev. Mol. Cell Biol. *21*, 341–352.

46. Piera-Velazquez, S., and Jimenez, S.A. (2019). Endothelial to mesenchymal transition: role in physiology and in the pathogenesis of human diseases. Physiol. Rev. *99*, 1281–1324.